Quantum noise and polarization fluctuations in vertical-cavity surface-emitting lasers

Holger F. Hofmann and Ortwin Hess
Institute of Technical Physics, DLR, Pfaffenwaldring 38-40, D-70569 Stuttgart, Germany
(Received 6 December 1996)

We investigate the polarization fluctuations caused by quantum noise in quantum-well vertical-cavity surface-emitting lasers (VCSELs). Langevin equations are derived on the basis of a generalized rate equation model in which the influence of competing gain-loss and frequency anisotropies is included. This reveals how the anisotropies and the quantum-well confinement effects shape the correlations and the magnitude of fluctuations in ellipticity and in the polarization direction. According to our results, all parameters used in the rate equations may be obtained experimentally from precise time-resolved measurements of the intensity and polarization fluctuations in the emitted laser light. To clarify the effects of anisotropies and of quantum-well confinement on the laser process in VCSELs we therefore propose time-resolved measurements of the polarization fluctuations in the laser light. In particular, such measurements allow us to distinguish the effects of frequency anisotropy and of gain-loss anisotropy and would provide data on the spin relaxation rate in the quantum-well structure during cw operation as well as representing a different way of experimentally determining the linewidth enhancement factor α. [S1050-2947(97)02307-X]

PACS number(s): 42.55.−f

I. INTRODUCTION

Vertical-cavity surface-emitting lasers (VCSELs) have recently attracted intensive experimental and theoretical effort. One of the major advantages VCSELs have over conventional semiconductor lasers is the highly symmetric geometry around the axis of laser light emission. The polarization of light emitted from VCSELs is therefore not determined by the massive anisotropy of the device architecture, as is the case in edge emitting lasers. Instead, due to the transverse symmetry of the cavity and the active region, the polarization is highly sensitive to more subtle effects, such as small anisotropies in the crystal structure, strain, or optical anisotropies in the mirrors [1–5].

Experiments have already provided a large range of results on polarization as a function of pumping current [4,6]. The variety of results indicates the sensitive dependence of polarization on very small effects. However, the connection between the observed stability or bistability of linear polarization and the theoretical explanations offered are still no more than tentative.

In 1995, San Miguel, Feng, and Moloney introduced a rate equation model for quantum well VCSELs that is based on the observation that the electron-hole pairs in the bands closest to the band gap can be separated into electron-hole pairs emitting only right circularly polarized light and electron-hole pairs emitting only left circularly polarized light [7]. Effectively, this corresponds to two independent reservoirs of electron hole pairs, each characterized by its own electron-hole pair density, coupled only by spin-relaxation processes. In the following, this assumption will be referred to as the ''split density model.''

The first major result derived from this model has been the proposal that polarization stability may be a consequence of a frequency anisotropy due to birefringence in the optical cavity [8]. As opposed to the more straightforward assumption of a gain-loss anisotropy, the frequency anisotropy may give rise to polarization switching as the injection current is increased. However, since polarization switching may also be induced by temperature-related effects [6], the fact that polarization switching is experimentally observed is not sufficient to verify the assumption of dominating frequency anisotropies. Although further work based on the split density model of San Miguel and co-workers has recently been put forth [5,9], the predictions made by the model have so far been insufficient to truly rule out the presence of alternative mechanisms. In particular, no attempts have yet been made to determine the anisotropies and the time scales involved in the laser process directly from the laser emission during cw operation.

In order to demonstrate that such a direct test of the model is indeed possible, we investigate the polarization fluctuations predicted by the Langevin equations derived from the split density model. One of the advantages of this approach is that polarization fluctuations can be measured at a fixed injection current during cw operation. Deriving the anisotropies from fluctuation measurements provides not only a tool for testing the theory, but can also provide information about temperature-dependent changes in the anisotropies. In this way, our theory may help to resolve questions such as those raised in [6] and [9].

In Sec. II of this paper, we formulate the full rate equations of the split density model using the normalized Stokes parameters to describe light field polarization. In Sec. III, we examine the most likely case of a frequency anisotropy and a gain-loss anisotropy along the same or two orthogonal crystal axes. The linearized Langevin equations for the stationary point are derived. In Sec. IV, the solution of the Langevin equation is given, using reasonable approximations with regard to the time scales involved. In Sec. V, the results are discussed and possible experiments are proposed. Finally, in Sec. VI, conclusions and an outlook are presented.

II. FORMULATION OF THE RATE EQUATIONS FOR THE SPLIT DENSITY MODEL

A. The split density model

If only the lowest-lying conduction bands and the highest-lying valence bands contribute to the laser process in a quantum-well structure, the preservation of angular momentum around the axis perpendicular to the quantum well and the fact that photons that are emitted along this axis have angular momenta of ± 1 (corresponding to either left or right circular polarization) limit the number of possible emission processes to two separate transitions. Conduction-band electrons with a spin of $+1/2$ around the axis perpendicular to the well can recombine only with heavy holes of $-3/2$ angular momentum around this axis, emitting a photon with an angular momentum of -1. (Note that a hole with an angular momentum of $-3/2$ corresponds to an empty electronic level with an angular momentum of $+3/2$.) Correspondingly, spin-1/2 electrons recombine only with holes of $+3/2$ angular momentum, emitting photons with an angular momentum of $+1$.

This means that effectively two completely distinct pools of electron-hole pairs exist. In one pool each electron-hole pair has an angular momentum of -1 and interacts only with right circularly polarized light. The electron-hole pairs in the other pool, having an angular momentum of $+1$ per pair, interact only with left circularly polarized light. Rate equations based on this assumption have been formulated originally by San Miguel and co-workers in [7]. In the following we adopt the notion of the split density model and considerably extend the analysis towards a generalized representation able to accommodate in the model arbitrary types of anisotropies.

B. Parameters

As in the paper by San Miguel *et al.* [7], we use the variables D for the total electron-hole density and d for the difference between the densities of electron-hole pairs with $+1$ and with -1 angular momentum. We will use a somewhat different approach to describe the light field in the cavity, however, to emphasize the difference between the light field intensity and light field polarization. The total number of photons in the cavity (regardless of polarization) is denoted by n. The polarization is then described by a three-dimensional vector of unit length **P**, which defines the point on the Poincaré sphere corresponding to the present polarization. The components of **P** are the normalized Stokes parameters. If $E_{\pm}$ are the complex electric-field amplitudes of right and left circular light, the normalized Stokes parameters are given by

$$P_1=\frac{E_+^*E_-+E_-^*E_+}{E_+^*E_++E_-^*E_-}, \tag{1a}$$

$$P_2=-i\frac{E_+^*E_--E_-^*E_+}{E_+^*E_++E_-^*E_-}, \tag{1b}$$

$$P_3=\frac{E_+^*E_+-E_-^*E_-}{E_+^*E_++E_-^*E_-}. \tag{1c}$$

The spatial directions of the vector **P** correspond to pairs of orthogonal polarizations. The component of **P** along any given direction is equal to the intensity difference between the two polarizations relative to the total intensity. P_3 is the intensity difference between left and right circular polarization, P_1 is the intensity difference between x and y polarization and P_2 is the intensity difference between light polarized along the (1,1) direction and light polarized along the $(1,-1)$ direction. In the plane of linear polarization, a rotation of **P** by 180° therefore corresponds to a 90° change in the direction of polarization. While this may not seem a very intuitive picture at first, one of the advantages of describing the light field in terms of **P** is that it directly refers to light field intensities as they are observed in experiment.

C. Time scales and anisotropies

The laser process in the split density model for quantum-well VCSELs is characterized by four time scales and three anisotropies. From slowest to fastest, the time scales are defined by (i) the rate of spontaneous emission into the laser mode $2w$, usually around 10^6–10^7 s^{-1}, although this can be very much a function of cavity design [10,11], (ii) the rate of spontaneous carrier decay γ, usually around 10^9–10^{10} s^{-1}, which also depends strongly on the cavity (in fact, the reduction of this decay into nonlaser modes is at the heart of a proposal to achieve thresholdless lasing by optimizing the optical cavity [11]); (iii) the rate of spin relaxation γ_s (this rate is an unknown quantity, especially in the high carrier density regime crucial to the laser structures under investigation; in this model, it appears only as the sum with the spontaneous carrier decay, which we define as $\Gamma=\gamma_s+\gamma$; experiments and theory indicate, however, that the order of magnitude will probably be similar to that of γ [12,13]; and (iv) the rate of photon emission from the cavity 2κ. The factor of 2 in the rate of spontaneous emission is a result of using photon number and intensity variables instead of the field amplitudes to describe the light in the cavity. Also, note that both w and κ are averages over anisotropic properties of the VCSEL.

The three possible anisotropies in gain, loss and frequency are characterized by both their magnitude and their geometrical orientation. Similar to the definition of the Stokes vector **P**, it is possible to represent the anisotropies by vectors. The direction of this vector corresponds to the direction of **P** for which the extremal gain, loss, and frequency values are obtained. The length corresponds to the difference between the extremal values. The anisotropy vectors are defined as gain anisotropy **g**, such that the rate of spontaneous emission is given by $2w(1+\mathbf{P}\cdot\mathbf{g})$; loss anisotropy ***l***, such that the rate of photon emission from the cavity is given by $2\kappa(1+\mathbf{P}\cdot\boldsymbol{l})$; and frequency anisotropy $\boldsymbol{\Omega}$, such that the length of Ω is equal to 1/2 the frequency difference between the modes of orthogonal polarization.

D. Rate equations

We can now formulate the rate equations for any arbitrary set of anisotropies using the parameters defined above:

$$\frac{d}{dt}D=-w(1+\mathbf{P}\cdot\mathbf{g})Dn-\gamma(D-D_0)-w(1+\mathbf{P}\cdot\mathbf{g})dnP_3, \tag{2a}$$

$$\frac{d}{dt}n=w(1+\mathbf{P}\cdot\mathbf{g})Dn-2\kappa(1+\mathbf{P}\cdot\mathbf{l})n+w(1+\mathbf{P}\cdot\mathbf{g})dnP_3, \tag{2b}$$

$$\frac{d}{dt}d=-w(1+\mathbf{P}\cdot\mathbf{g})dn-\Gamma d-w(1+\mathbf{P}\cdot\mathbf{g})DnP_3, \tag{2c}$$

$$\frac{d}{dt}\mathbf{P}=\{[w(1+\mathbf{P}\cdot\mathbf{g})(D\mathbf{g}+d\hat{\mathbf{e}}_3)-2\kappa(1+\mathbf{P}\cdot\boldsymbol{l})\boldsymbol{l}]\times\mathbf{P}\}\times\mathbf{P}$$
$$+[\boldsymbol{\Omega}+w(1+\mathbf{P}\cdot\mathbf{g})\alpha d\hat{\mathbf{e}}_3]\times\mathbf{P}. \tag{2d}$$

$\hat{\mathbf{e}}_3$ indicates the unit vector in the direction of the third component of the Stokes vector.

D_0 is the injection current in units of γ and α is the linewidth enhancement factor, which describes a shift in frequency due to the electron-hole density in the quantum well. In the presence of two separate reservoirs of electron-hole pairs (split density model), where the carriers from one reservoir interact with only one type of circular polarization, the frequency shift causes an effective birefringence [8].

To understand the terms in the equation, it is important to keep in mind that each time κ and w appear in the equations, they are modified by the anisotropy factors of $(1+\mathbf{P}\cdot\boldsymbol{l})$ and $(1+\mathbf{P}\cdot\mathbf{g})$, respectively. In the model this is the only influence of the anisotropies on the dynamics of D and n if $d=0$. If $d\neq 0$, the last terms in Eqs. (2a) and (2b) increase or decrease the rate of stimulated emission, depending on whether the light field in the cavity interacts more strongly or more weakly with the available carriers. The last term in Eq. (2c) describes the hole burning effect of $P_3\neq 0$.

The dynamics of the Stokes parameters $\mathbf{P}$ is directly determined by the anisotropies. The frequency anisotropy induces a rotation around the axis defined by $\boldsymbol{\Omega}$. The gain-loss anisotropy draws $\mathbf{P}$ towards one of the poles along the axis defined by $\mathbf{g}$ and $\boldsymbol{l}$, at a rate proportional to the component of $\mathbf{g}$ or $\boldsymbol{l}$ orthogonal to $\mathbf{P}$. This is illustrated in Fig. 1.

The effect of the split density model on the polarization dynamics can be understood in terms of gain and frequency anisotropies introduced by the density difference d:

$$\mathbf{g}_{eff}=\mathbf{g}+\frac{d}{D}\hat{\mathbf{e}}_3 \tag{3}$$

$$\boldsymbol{\Omega}_{eff}=\boldsymbol{\Omega}+w(1+\mathbf{P}\cdot\mathbf{g})\alpha d\hat{\mathbf{e}}_3. \tag{4}$$

In passing we note that another consequence of the split density model is the fact that the factor of 2 in the rate of spontaneous emission is absent. This is due to the two parallel laser processes having an induced emission rate of $2w(D/2)(n/2)$ for $d=0$ and $P_3=0$. The sum of the two emission rates is therefore wDn, as given above.

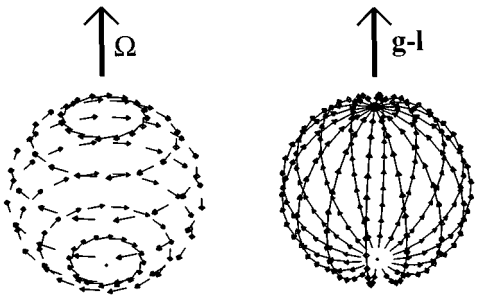

FIG. 1. Arrows on the Poincaré spheres illustrate the dynamical effect of anisotropies on the normalized Stokes vector $\mathbf{P}$. The sphere on the left shows how the frequency anisotropy causes $\mathbf{P}$ to rotate around the axis defined by the anisotropy. The sphere on the right shows how the gain-loss anisotropy pulls $\mathbf{P}$ towards one of the poles defined by the vector of anisotropy.

III. LANGEVIN EQUATIONS FOR cw OPERATION AT A STABLE LINEAR POLARIZATION

A. Anisotropies along the [110] and [1$\bar{1}$0] crystal axes

Although a large number of nonlinear effects and dynamical properties can be described by choosing special combinations of anisotropies [9], we will concentrate on the simple case of cw operation at a stable linear polarization. For many VCSELs, this seems to be the natural state of affairs, even when no artificial anisotropies were created during the growth of the device. It has been found that a large number of VCSELs emit light polarized along the [110] or [1$\bar{1}$0] crystal axis [1–5]. This must obviously be the result of unintentionally introduced anisotropies. Possible reasons for this are the slight tilt of the growth axis often used in metal-organic chemical-vapor deposition [4] or the tendency of strain induced changes in the optical properties to produce anisotropies along these axes [5]. The latter effect can be visualized quite nicely. If one looks at a [001] surface of a semiconductor lattice, the projections of the bonds appear along the [110] and the [1$\bar{1}$0] directions. Light polarized along one of these directions will mainly interact with the electrons in the bonds along this direction. Consequently, the largest part of the optical anisotropy induced by stress is caused by the difference in compression between the [110] and the [1$\bar{1}$0] bond directions.

Given this preference for two orthogonal linear polarizations observed in many VCSELs, we choose $\mathbf{g}=g\hat{\mathbf{e}}_1$, $\boldsymbol{l}=l\hat{\mathbf{e}}_1$, and $\boldsymbol{\Omega}=\Omega\hat{\mathbf{e}}_1$. The rate equations are now

$$\frac{d}{dt}D=-w(1+P_1g)Dn-\gamma(D-D_0)-w(1+P_1g)dnP_3, \tag{5a}$$

$$\frac{d}{dt}n=w(1+P_1g)Dn-2\kappa(1+P_1l)n+w(1+P_1g)dnP_3, \tag{5b}$$

$$\frac{d}{dt}d=-w(1+P_1g)dn-\Gamma d-w(1+P_1g)DnP_3, \tag{5c}$$

$$\frac{d}{dt}P_1=-[w(1+P_1g)Dg-2\kappa(1+P_1l)l](P_1^2-1) - w(1+P_1g)d(P_3P_1-\alpha P_2), \tag{5d}$$

$$\frac{d}{dt}P_2=-[w(1+P_1g)Dg-2\kappa(1+P_1l)l]P_1P_2 - w(1+P_1g)d(P_3P_2+\alpha P_1)-\Omega P_3, \tag{5e}$$

$$\frac{d}{dt}P_3=-[w(1+P_1g)Dg-2\kappa(1+P_1l)l]P_1P_3 - w(1+P_1g)d(P_3^2-1)+\Omega P_2. \tag{5f}$$

B. Linearization around the stationary solution

The stationary solution of these equations is given by $P_1=1$, $P_2=P_3=d=0$, and $D=2\kappa(1+l)/w(1+g)$. The photon number in the cavity n_s is a linear function of D_0, specifically

$$n_s=\frac{\gamma}{2\kappa(1+l)}D_0-\frac{\gamma}{w(1+g)}. \tag{6}$$

Close to this stationary point the laser relaxation dynamics can be linearized. Deviations from the stationary point are described by five coupled dynamical variables. In the case under consideration the dynamics can be seperated into two mutually decoupled subsystems. One subsystem describes the dynamics of the total photon number fluctuations $\delta n=n-n_s$ coupled to the total density fluctuations $\delta D=D-2\kappa(1+l)/w(1+g)$. The other subsystem describes the coupling of the density difference d to the polarization parameters P_2 and P_3.

To obtain the linearized Langevin equation, we further add the noise term $\mathbf{f}(t)$ to the dynamics. This time-dependent five-dimensional vector incorporates all external noise and signals influencing the laser. In the case under consideration, this will be the vacuum fluctuations of the light field entering the cavity. A discussion of the statistical properties of this noise term will be given in Sec. III C.

At this point, it is convenient to introduce five new parameters for a more compact formulation

(i) The injection current in units of the threshold current is defined as x, which means that the stationary photon number n_s is replaced by

$$x=\frac{w(1+g)}{\gamma}n_s+1. \tag{7}$$

(ii) The gain-loss anisotropy is combined into a single variable ρ equal to the difference of the two, scaled with the ratio of the cavity loss rate and spontaneous carrier decay. This dimensionless quantity should be of the order of unity to be effective, corresponding to a relative anisotropy of about 0.1% for typical time scales:

$$\rho=\frac{2\kappa(1+l)}{\gamma}(g-l). \tag{8}$$

(iii) The frequency anisotropy is scaled in terms of the spontaneous carrier decay rate divided by α, as it only stabilizes the polarization in conjunction with α [8]:

$$\theta=\frac{\alpha\Omega}{\gamma}. \tag{9}$$

(iv) The ratio of the spin-relaxation rate and spontaneous carrier decay rate is written as r, such that

$$r=\frac{\Gamma}{\gamma}-1. \tag{10}$$

(v) The relaxation oscillation frequency ν is defined as a function of the injection current x:

$$\nu=\sqrt{2\kappa(1+l)\gamma(x-1)}. \tag{11}$$

Using these parameters, the Langevin equation for the quantum-well VCSEL is

$$\frac{d}{dt}\begin{pmatrix}\delta D\\ \delta n\\ d\\ P_2\\ P_3\end{pmatrix}=\begin{pmatrix}-\gamma x & -\frac{\nu^2}{\gamma(x-1)} & 0 & 0 & 0\\ \gamma(x-1) & 0 & 0 & 0 & 0\\ 0 & 0 & -\gamma(x+r) & 0 & \frac{\nu^2}{w(1+g)}\\ 0 & 0 & -w(1+g)\alpha & -\gamma\rho & -\frac{\gamma\theta}{\alpha}\\ 0 & 0 & -w(1+g) & \frac{\gamma\theta}{\alpha} & -\gamma\rho\end{pmatrix}\begin{pmatrix}\delta D\\ \delta n\\ d\\ P_2\\ P_3\end{pmatrix}+\mathbf{f}(t). \tag{12}$$

All processes described by this equation occur either at a rate of γ or at a rate of ν. Since it is realistic to assume that $\gamma \ll \kappa$, the spontaneous carrier decay rate γ will usually be significantly smaller than the relaxation oscillation frequency $\nu = \sqrt{2\kappa(1+l)\gamma(x-1)}$. Note that this condition breaks down very close to threshold ($x=1$). However, as close to threshold the relative polarization fluctuations approach infinity, there is no polarization stability for x very close to one.

C. Quantum noise

Although the formulation given above can be applied also to problems of externally injected fields and similar linear response problems, we will now define the noise term $\mathbf{f}(t)$ as the electromagnetic field noise entering the cavity from the vacuum. The definition of a noise term for the light field in a cavity is a standard procedure in quantum optics. In the case of two modes of orthogonal polarization, the extension is straightforward. The two-time correlation functions that are nonzero are

$$\langle f_{\delta n}(t) f_{\delta n}(t+\tau)\rangle = 4\kappa(1+l)n_s\delta(\tau) = \frac{4\kappa(1+l)\gamma(x-1)}{w(1+g)}\delta(\tau), \quad (13a)$$

$$\langle f_{p_2}(t) f_{p_2}(t+\tau)\rangle = \frac{4\kappa(1+l)}{n_s}\delta(\tau) = \frac{4\kappa(1+l)w(1+g)}{\gamma(x-1)}\delta(\tau), \quad (13b)$$

$$\langle f_{p_3}(t) f_{p_3}(t+\tau)\rangle = \frac{4\kappa(1+l)w(1+g)}{\gamma(x-1)}\delta(\tau). \quad (13c)$$

To understand the derivation of these terms, either one may think in terms of a classical field, considering the vacuum modes and the dipole densities associated with the carrier density pools as field modes with random quantum fluctuations acting as external forces on the field in the cavity, or one may apply particle picture reasoning: Since only whole photons are emitted into and out of the cavity, there is a stochastic process involved that gives rise to shot noise. It is one of the fascinating properties of quantum mechanics that the same noise terms result from two seemingly different pictures.

Another noise source for the laser process is the noise in the carrier injection. However, this noise is much weaker than the light field noise if $\gamma x \ll \kappa$, which is a natural assumption for real devices. The physical reason for the relative smallness of shot noise from injection is that if the photon emission rate from the cavity is much faster than the total carrier decay rate, then the number of carriers present in the active region is far greater than the number of photons in the cavity. Consequently, the relative statistical fluctuations are much smaller in the carrier subsystem than in the light field.

Note that this approximation is valid only for short time scales. On time scales much longer than the $1/\gamma$, energy conservation requires the fluctuations described here to cancel. This means that the low-frequency noise of the power spectrum is very sensitive to the weak fluctuations in the carrier injection [15].

IV. SOLUTION OF THE LANGEVIN EQUATION

A. The Green's function solution near the stationary point

In accordance with the fluctuation-dissipation theorem, the noise in the light emitted from the laser is approximately given by a linear response to the quantum noise entering the laser cavity. The fluctuations can therefore be calculated from the linear response of the VCSEL. The five-dimensional Green's function can be obtained by determining the eigenvalues and eigenvectors of the nonsymmetric 5×5 matrix describing the linearized dynamics. Since the eigenvectors are nonorthogonal, both left and right eigenvectors need to be determined.

The problem separates into one two-dimensional problem and one three-dimensional problem. Therefore, an exact analytical solution is possible. However, to understand the physical significance and to single out the experimentally relevant case, it is useful to apply the realistic assumption that since $\gamma x \ll \kappa$, $\gamma \ll \nu$, except for x very close to 1. Also, the anisotropies ρ and θ should not be much greater than 1. Using these assumptions, the eigenvalues λ_i and eigenvectors $\mathbf{a}_i$ and $\mathbf{b}_i$ are

$$\lambda_{1/2} = -\frac{1}{2}\gamma x \pm i\nu,$$

$$\mathbf{a}_{1/2} = \frac{1}{\sqrt{2}}\left(\mp i\frac{\gamma(x-1)}{\nu}1000\right), \quad \mathbf{b}_{1/2} = \frac{1}{\sqrt{2}}\begin{pmatrix} \pm i\dfrac{\nu}{\gamma(x-1)} \\ 1 \\ 0 \\ 0 \\ 0 \end{pmatrix}; \quad (14)$$

$$\lambda_3 = -\gamma(\rho+\theta),$$

$$\mathbf{a}_3 = (0001-\alpha), \quad \mathbf{b}_3 = \begin{pmatrix} 0 \\ 0 \\ 0 \\ 1 \\ 0 \end{pmatrix}; \quad (15)$$

$$\lambda_{4/5} = -\frac{1}{2}\gamma(x+r+\rho-\theta) \pm i\nu,$$

$$\mathbf{a}_{4/5} = \frac{1}{\sqrt{2}}\left(00\mp i\frac{w(1+g)}{\nu}01\right), \quad \mathbf{b}_{4/5} = \frac{1}{\sqrt{2}}\begin{pmatrix} 0 \\ 0 \\ \pm i\dfrac{\nu}{w(1+g)} \\ \alpha \\ 1 \end{pmatrix}. \quad (16)$$

Using this set of vectors, any external perturbation of field variables or carrier densities can be decomposed into the eigenvectors with the corresponding exponentially decaying and oscillating Green's function. The time integral over the perturbation then gives the linear response of the laser dynamics. This procedure can now be applied to quantum noise.

B. Application of the Green's function to quantum noise

The left eigenvectors $\mathbf{a}_i$ are used to decompose the noise into contributions associated with the corresponding eigenvalues. If the noise terms are represented in the form of a 5×5 diffusion matrix $\mathbf{N}$ [14], the decomposition can be accomplished by calculating the matrix elements $N_{i,j}=\mathbf{a}_i\mathbf{N}\mathbf{a}_j^{\dagger}$. The fluctuation matrix $\mathbf{F}(\tau)$ can then be expressed as a sum over the dyadic products of the right eigenvectors $\mathbf{b}_i$,

$$\mathbf{F}(\tau)=\sum_{i,j}\frac{N_{i,j}}{-\lambda_i-\lambda_j^*}e^{\lambda_j^*\tau}\mathbf{b}_i\otimes\mathbf{b}_j^{\dagger}. \tag{17}$$

As the eigenvectors are not orthogonal, there are contributions for $i\neq j$ with complex $-\lambda_i-\lambda_j^*$. Since we apply the approximation that $\gamma\ll\nu$, however, the absolute value of these terms is much smaller than those with $i=j$ and we can obtain the light field fluctuations by summing over the five terms with $i=j$ only. This effectively means that the eigenvectors fluctuate independently. The fluctuation matrix is then given by a sum over projection operators that must be symmetric.

C. Light field fluctuations

The light field fluctuations of polarized light have three degrees of freedom, given by the total intensity n, the ellipticity P_3, and the direction of linear polarization P_2. Including possible correlations, these fluctuations are described by a symmetric 3×3 matrix. However, since the dynamics of the total intensity is decoupled from the polarization dynamics, there is no correlation between the total intensity and the polarization. Therefore, four fluctuation terms are sufficient to completely describe the fluctuations in the laser light during cw operation:

$$\langle\delta n(t)\,\delta n(t+\tau)\rangle=\frac{2\kappa(1+l)}{w(1+g)}\frac{x-1}{x}e^{-\gamma x\tau/2}\cos(\nu\tau), \tag{18}$$

$$\frac{\langle\delta n(t)\,\delta n(t+\tau)\rangle}{n_s^2}=\frac{A}{x(x-1)}e^{-\gamma x\tau/2}\cos(\nu\tau), \tag{19}$$

$$\langle P_3(t)P_3(t+\tau)\rangle=\frac{A}{(x-1)(x+r+\rho-\theta)}e^{-\gamma(x+r+\rho-\theta)\tau/2}\cos(\nu\tau), \tag{20}$$

$$\langle P_3(t)P_2(t+\tau)\rangle=\alpha\langle P_3(t)P_3(t+\tau)\rangle=\frac{\alpha A}{(x-1)(x+r+\rho-\theta)}e^{-\gamma(x+r+\rho-\theta)\tau/2}\cos(\nu\tau), \tag{21}$$

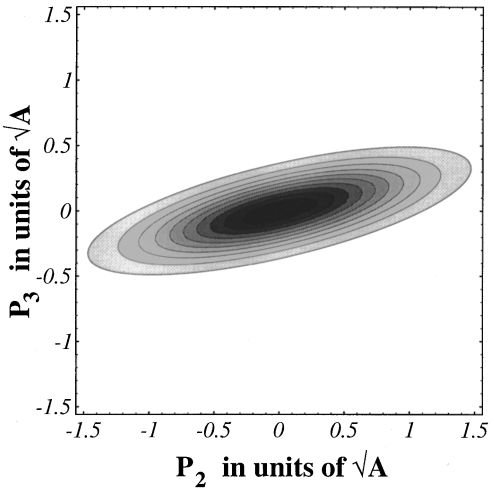

FIG. 2. Contour plot of the Gaussian distribution corresponding to the polarization fluctuations at $\tau=0$ for $x=2$, $\alpha=2$, $r=2$, $\rho=2$, and $\theta=2$. This choice of parameters clearly shows the correlation between polarization direction and ellipticity. For $A=0.01$, the fluctuations of P_2 correspond to deviation of approximately $\pm5°$ in the direction of polarization.

$$\langle P_2(t)P_2(t+\tau)\rangle=\frac{\alpha^2A}{(x-1)(x+r+\rho-\theta)}e^{-\gamma(x+r+\rho-\theta)\tau/2}\cos(\nu\tau)+\frac{A(1+\alpha^2)}{(x-1)(\rho+\theta)}e^{-\gamma(\rho+\theta)\tau}. \tag{22}$$

The factor A is a measure of the overall magnitude of noise

$$A=\frac{2\kappa(1+l)w(1+g)}{\gamma^2}. \tag{23}$$

Figure 2 shows the noise distribution at $\tau=0$ for a realistic choice of parameters. Figure 3 shows the polarization fluctuations as a function of τ.

There is a correlation between the two fluctuations, mediated by α, which is a typical feature of the two-density model. The α factor converts the density difference fluctuations d into frequency difference fluctuations between left and right circular polarization. This fluctuating birefringence causes the direction of polarization to fluctuate in phase with the ellipticity. The fluctuations of the carrier density have not been given here since they are difficult to observe experimentally. They would be strongly correlated with the oscillating field terms, being 90° out of phase with respect to the fluctuations of the field.

Because of this correlation effect, fluctuations in the direction of polarization P_2 are always much stronger than fluctuations in the ellipticity P_3 if α is greater than 1. Indeed, the values of 2–6 given for α in the literature suggest a difference of almost an order of magnitude.

Another typical feature of the polarization fluctuations is that they approach infinity close to threshold. This is an indicator that the light emitted very close to threshold is still

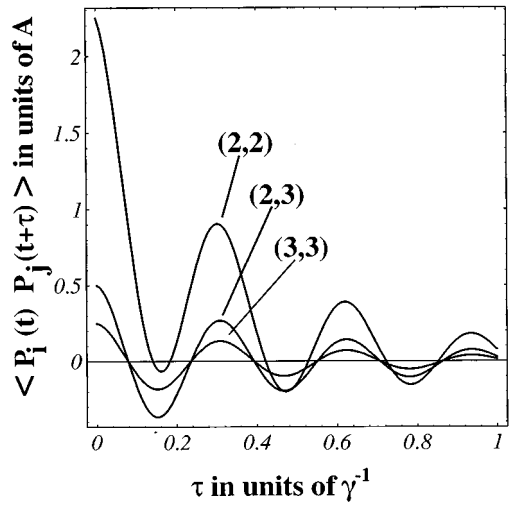

FIG. 3. Time dependence of the fluctuations $\langle P_i(t)P_j(t+\tau)\rangle$ for $x=2$, $\alpha=2$, $r=2$, $\rho=2$, and $\theta=2$. As explained in the text, the fluctuation of polarization direction $(i,j)=(2,2)$ is largest, while the correlation of polarization direction and ellipticity $(i,j)=(2,3)$ is exactly equal in magnitude to two times the fluctuations in ellipticity $(i,j)=(3,3)$. Time is given in units of γ^{-1}, which is typically 100 ps to 1 ns. The variable A is typically around 1/100.

lamplike. A nonvanishing amount of laser emission is necessary to overcome the noise effects and to stabilize both the intensity and the polarization.

Although three unknown parameters r, ρ, and θ enter into the model, the polarization noise terms calculated here are defined by only two parameters, namely, $\rho+\theta$ and $r+\rho-\theta$. To fully separate the effects of spin relaxation and of anisotropy, one additional parameter is needed. This additional parameter may be found by taking a closer look at the nearly degenerate oscillation frequencies in the intensity and in the polarization.

D. Perturbation theory for the frequency of relaxation oscillations

The relaxation oscillations appear equally in the total intensity and in the polarization fluctuations. This is a direct result of the two-density model: Ellipticity fluctuations and the associated fluctuations in the polarization direction are a result of uncorrelated intensity fluctuations in the two circular polarizations.

However, anisotropies couple the two subsystems and induce slight changes in the frequency. By calculating the difference between the relaxation oscillations in intensity and in polarization, further information on the anisotropies can be obtained.

The perturbative correction to the eigenvalues may be obtained by calculating the matrix elements $M_{i,j}$ between the approximate eigenvectors $\mathbf{a}_i$ and $\mathbf{b}_j$. The correction to the eigenvalue λ_i caused by a weak coupling to the eigenstates of λ_j is given by $M_{i,j}M_{j,i}/(\lambda_i-\lambda_j)$. Calculated to second order in γ/ν, the eigenvalue corrections are

$$\delta\lambda_1=\frac{M_{1,2}M_{2,1}}{\lambda_1-\lambda_2}$$

$$=-i\frac{\gamma^2x^2}{8\nu}, \tag{24}$$

$$\delta\lambda_2=-\delta\lambda_1 \tag{25}$$

for the total photon number and

$$\delta\lambda_3=0, \tag{26}$$

$$\delta\lambda_4=\frac{M_{4,5}M_{5,4}}{\lambda_4-\lambda_5}+\frac{M_{4,3}M_{3,4}}{\lambda_4-\lambda_3}$$

$$=-i\frac{\gamma^2}{8\nu}(x+r-\rho+\theta)^2$$

$$+i\frac{\gamma^2\theta^2(\alpha^2+1)}{2\nu}, \tag{27}$$

$$\delta\lambda_5=-\delta\lambda_4 \tag{28}$$

for the polarization variables. The difference in frequency between the intensity oscillations ν_n and the polarization oscillations ν_P is

$$\nu_n-\nu_P=\frac{\gamma^2}{8\nu}\left[(x+r-\rho+\theta)^2-x^2-4\theta^2\frac{\alpha^2+1}{\alpha^2}\right]. \tag{29}$$

Note that only a frequency anisotropy will make ν_P larger than ν_n. Therefore, if the polarization noise oscillates faster than the intensity noise, this is an indicator of a strong frequency anisotropy.

V. DISCUSSION OF THE RESULTS AND EXPERIMENTAL POSSIBILITIES

A. Determination of time scales and anisotropies from the fluctuations of the laser light

The equations given above show the wealth of information that can be obtained from measurements of the fluctuations in the laser light emitted from a VCSEL during cw operation at a stable linear polarization. Intensity noise is given by the relaxation rate $\gamma x/2$, the oscillation frequency ν, and the relative magnitude of $A/x(x-1)$. The experimental determination of these three quantities is equivalent to a measurement of the three time scales $\kappa(1+l)$, γ, and $w(1+g)$.

The ellipticity noise $\langle P_3(t)P_3(t+\tau)\rangle$ differs from intensity noise in the relaxation rate, which is $\gamma(x+r+\rho-\theta)/2$ instead of $\gamma x/2$, and in the relaxation frequency, although the latter is only slightly different. These time scales also show up in the correlation of ellipticity and polarization direction fluctuations $\langle P_3(t)P_2(t+\tau)\rangle$, which is just α times the ellipticity fluctuations. An observation of this correlation can not only provide strong evidence in support of the split density model, but is also a direct measurement of α. Finally, the fluctuations of polarization direction $\langle P_2(t)P_2(t+\tau)\rangle$ include not only noise correlated to ellipticity fluctuations, but

also additional noise with a relaxation rate of $\gamma(\rho+\theta)$. From the two relaxation rates and the difference in oscillation frequency, the parameters r, ρ, and θ can be calculated, thereby allowing an experimental determination of the spin relaxation rate, the gain-loss aniosotropy, and the frequency anisotropy.

B. Polarization stability

The polarization fluctuations predicted by the split density model are largely fluctuations of the direction of linear polarization. Fluctuations of the ellipticity are smaller by at least a factor of α^2. For very small anisotropies, the main contribution to the fluctuations will be from the weak relaxation rate of $\gamma(\rho+\theta)$, implying an even greater discrepancy between fluctuations in ellipticity and in polarization direction.

To estimate the relative anisotropies necessary to stabilize polarization, it is therefore most appropriate to require the condition $\rho+\theta \gg A(1+\alpha^2)/(x-1)$ to be fulfilled. For reasonable estimates, ρ and θ should then be at least of order 1. This would necessitate a relative gain-loss anisotropy $g-l$ of at least 10^{-3} or a frequency anisotropy of at least 1 GHz.

However, these values depend critically on the time scales of the laser process, all of which enter into the magnitude of the fluctuations given by A.

C. Experimental possibilities

To determine the time scales and the anisotropies of quantum-well VCSELs as described above, time-resolved measurements of the polarization fluctuations at a resolution of at least picoseconds are required. Further, polarization filters for both linear and circular polarization are needed.

Ideally, P_2 and P_3 could be measured directly by separating the laser beam using a birefringent material and measuring the intensity difference between the two parts. However, it is also possible to measure the fluctuations by inserting a filter and measuring the fluctuations in $n_s(1+P_{2/3})/2$. Since the fluctuations in n are not correlated with the fluctuations in polarization, the resulting relative noise is just the avarage of total intensity noise and polarization noise. For example, if one measures the fluctuations in the intensity of right circularly polarized light $I_+(t)$ one obtains

$$\frac{\langle I_+(t)I_+(t+\tau)\rangle}{\overline{I_+}^2}=\frac{1}{2}\left(\frac{\langle n(t)n(t+\tau)\rangle}{n_s^2}+\langle P_3(t)P_3(t+\tau)\rangle\right). \tag{32}$$

A measurement of the correlation of ellipticity and polarization direction fluctuations is very difficult since it requires a splitting of the laser beam without causing undesireable polarizations. Probably the best approach would be to reflect only a small fraction of the beam at a right angle, using this light for the measurement of the linear polarization direction and using the nearly unaltered beam for the measurement of ellipticity fluctuations. Another possibility is to keep track of all the polarization properties of the optical devices used, sorting out the contributions to the measured noise afterward. The Stokes parameters are quite convenient for this task since all polarization effects can be described by matrix multiplication.

In this manner, all time scales and anisotropies can be determined at a fixed injection current. If such an experiment works, it is also possible to measure changes in these properties as injection current is increased. A comparison with the temperature dependence at constant injection current is also possible. This should reveal many of the material properties of the semiconductor and help to clear up some of the open questions regarding polarization switching.

VI. CONCLUSIONS AND OUTLOOK

The analysis presented here shows how all the parameters of the two-density model for a VCSEL with stable linear polarization can be obtained from measurements of the polarization fluctuations. Time-resolved measurements of the polarization fluctuations in VCSEL light can therefore unambiguously resolve open questions, such as whether temperature effects cause polarization switching or whether birefringence or gain-loss anisotropies are responsible for polarization stability.

This is extremely important because experimental results on polarization and intensity as a function of the injection current can be interpreted only when the correct mechanism of polarization stability has been identified. For example, the authors of [5] assume that only a frequency anisotropy contributes to polarization stability without considering the possibility that a gain-loss anisotropy might have an effect as well. Unverified assumptions are also the subject of the criticism voiced in [9] about the explanations given in [6]. Further experiments such as the ones proposed here are absolutely necessary to avoid misleading interpretations.

The polarization fluctuations show features typical for the split density model, which can be used as a test criterion for whether or not the model is valid in a given device. Since the split density represents the effect of quantum-well confinement on the polarization properties of VCSELs, this effectively tests the quantum-well structure in the active region. The quantity that depends strongly on the size of the quantum wells is the spin-relaxation rate. Experimental results on this rate are also of interest in connection with calculations [12,16] and luminesence experiments [13] carried out to investigate spin-flip scattering in quantum wells.

The rate equations presented here are formulated in a very general way and may also be applied to cases with more excotic anisotropies and time scales, such as discussed in [8] and [9], which show switching and/or include a magnetic field. In all these cases, the investigation of noise adds additional predictions for experiment to the results and thereby increases our understanding of the physics involved in the polarization properties of VCSELs.

[1] C. J. Chang-Hasnain *et al.*, IEEE J. Quantum Electron. **27**, 1402 (1991).
[2] F. Koyama, K. Morito, and K. Iga, IEEE J. Quantum Electron. **QE-27**, 1410 (1991).
[3] D. Vakhshoori, Appl. Phys. Lett. **65**, 259 (1995).
[4] K. D. Choquette, R. P. Schneider, K. L. Lear, and R. E. Leibenguth, IEEE J. Selec. Topics **1**, 661 (1995).
[5] A. K. J. van Doorn, M. P. van Exter, and J. P. Woerdman, Appl. Phys. Lett. **69**, 1041 (1996).
[6] K. D. Choquette, D. A. Richie, and R. E. Leibenguth, Appl. Phys. Lett. **64**, 2062 (1994).
[7] M. S. Miguel, Q. Feng, and J. V. Moloney, Phys. Rev. A **52**, 1728 (1995).
[8] J. Martin-Regalado, M. S. Miguel, N. B. Abraham, and F. Prati, Opt. Lett. **21**, 351 (1995).
[9] M. Travagnin, M. P. van Exter, A. K. J. van Doorn, and J. P. Woerdman, Phys. Rev. A **54**, 1647 (1996).
[10] T. Baba, T. Hamano, F. Koyama, and K. Iga, IEEE J. Quantum Electron. **27**, 1347 (1991).
[11] H. Hirayama, T. Hamano, and Y. Aoyagi, Appl. Phys. Lett. **69**, 791 (1996).
[12] T. Uenoyama and L. J. Sham, Phys. Rev. B **42**, 7114 (1990).
[13] A. Vinattieri *et al.*, Phys. Rev. B **50**, 10 868 (1994).
[14] D. F. Walls and G. J. Milburn, *Quantum Optics* (Springer-Verlag, Berlin, 1995).
[15] Y. Yamamoto, S. Machida, and O. Nilsson, Phys. Rev. A **34**, 4025 (1986).
[16] R. Ferreira and G. Bastard, Phys. Rev. B **43**, 9687 (1991).